

1 **July 28, 2019**

2 **Termite mounds contain distinct methanotroph**
3 **communities that are kinetically adapted to elevated**
4 **methane concentrations**

5 **Eleonora Chiri^{1,2 #}, Chris Greening^{2 *}, Stefan K. Arndt^{1 *}, Philipp A. Nauer^{1,3 #}**

6

7 ¹ School of Ecosystem and Forest Sciences, University of Melbourne, Richmond, VIC
8 3121, Australia

9 ² School of Biological Sciences, Monash University, Clayton, VIC 3800, Australia

10 ³ School of Chemistry, Monash University, Clayton VIC 3800, Australia

11

12 [#] These authors contributed equally to this work.

13

14 ^{*} Correspondence can be addressed to:

15

16 Prof Stefan Arndt (sarndt@unimelb.edu.au), School of Ecosystem and Forest Sciences,
17 University of Melbourne, Richmond, VIC 3121, Australia

18 A/Prof Chris Greening (chris.greening@monash.edu), School of Biological Sciences,
19 Monash University, Clayton, VIC 3800, Australia

20 **Abstract**

21 Termite mounds have recently been confirmed to mitigate approximately half of termite
22 methane (CH_4) emissions, but the aerobic methane-oxidizing bacteria (methanotrophs)
23 responsible for this consumption have not been resolved. Here we describe the
24 abundance, composition, and kinetics of the methanotroph communities in the mounds
25 of three distinct termite species. We show that methanotrophs are rare members of the
26 termite mound biosphere and have a comparable abundance, but distinct composition, to
27 those of adjoining soil samples. Across all mounds, the most abundant and prevalent
28 particulate methane monooxygenase sequences detected were affiliated with Upland Soil
29 Cluster α (USC α), with sequences homologous to *Methylocystis* and Tropical Upland Soil
30 Cluster also detected. The Michaelis-Menten kinetics of CH_4 oxidation in mounds were
31 estimated from *in situ* reaction rates. The apparent CH_4 affinities of the communities were
32 in the low micromolar range, which is one to two orders of magnitude higher than those
33 of upland soils, but significantly lower than those measured in soils with a large CH_4
34 source such as landfill-cover soils. The rate constant of CH_4 oxidation, as well as the
35 porosity of the mound material, were significantly positively correlated with the abundance
36 of methanotroph communities of termite mounds. We conclude that termite-derived CH_4
37 emissions have selected for unique methanotroph communities that are kinetically
38 adapted to elevated CH_4 concentrations. However, factors other than substrate
39 concentration appear to limit methanotroph abundance and hence these bacteria only
40 partially mitigate termite-derived CH_4 emissions. Our results also highlight the
41 predominant role of USC α in an environment with elevated CH_4 concentrations and
42 suggest a higher functional diversity within this group than previously recognised.

43

44 Introduction

45 Termites are mound-building eusocial insects that live in colonies throughout the tropics
46 and subtropics. These organisms completely degrade lignocellulose in a process
47 primarily mediated by anaerobic symbiotic microorganisms in their hindgut [1]. During this
48 process, hydrogenotrophic methanogens produce substantial amounts of methane (CH_4)
49 that is emitted from the termite into the atmosphere [2–4]. Production rates vary by three
50 to four orders of magnitude depending on the termite species and their dietary
51 preferences (i.e. wood-, grass-, soil- or fungus-feeding) [1, 4, 5]. Current models suggest
52 that termites are responsible for between 1 to 3 % of global CH_4 emissions to the
53 atmosphere [6].

54 Aerobic methane-oxidizing bacteria (methanotrophs) significantly mitigate emissions of
55 CH_4 from termites [7]. Methanotrophs gain carbon and energy by oxidising CH_4 to carbon
56 dioxide, with the first step in this reaction being catalysed by particulate and soluble
57 methane-monooxygenases [8]. It is controversial whether termite hindguts harbor such
58 organisms; while *Methylocystis* spp. were recently isolated from termites [9], other studies
59 could not detect methanotroph functional gene markers or measurable amounts of $^{14}\text{CO}_2$
60 during $^{14}\text{CH}_4$ incubation experiments [10]. We also observed that the addition of inhibitors
61 of CH_4 oxidation did not increase direct termite CH_4 emissions [7]. However, many termite
62 colonies construct large mounds built from soil material or build their nest in soil, which is
63 generally a sink for atmospheric CH_4 [11]. While results from incubation experiments of
64 mound material were conflicting [12–14], we recently presented clear evidence of
65 widespread CH_4 oxidation in North Australian termite mounds [7]: results from three
66 different *in situ* methods to measure CH_4 oxidation in mounds confirmed that
67 methanotrophs mitigate between 20 to 80 % of termite-derived CH_4 before emission to
68 the atmosphere. However, the community composition and kinetic behaviour of the
69 methanotrophs responsible remain largely unknown.

70 Compared to soils, methanotrophs inhabiting termite mounds have received little
71 attention. Ho et al. [14] investigated mound material of the African fungus-feeding termite
72 *Macrotermes falciger* using a *pmoA*-based diagnostic microarray approach. Community
73 composition differed between mound and soil, and at some locations within the large

74 compartmentalised mounds. Slurry incubations confirmed potential CH₄ oxidation at high
75 and low CH₄ concentrations. The mound community was reportedly dominated by
76 gammaproteobacterial methanotrophs of the JR3 cluster, while the functional gene of the
77 soluble methane-monooxygenase could not be detected, nor could methanotrophs of the
78 Verrucomicrobia and Methylomirabilota (NC10) phyla. Beside this pioneering work, the
79 mound methanotroph communities of no other termite species has been investigated.
80 However, large differences might exist between termite species and particularly their
81 dietary preferences, as well as the mounds' impressive variety of sizes, shapes and
82 internal structures [15, 16]. Reflecting this, *in situ* studies have shown that there is a large
83 variation in methanotroph activity in mounds both within and between species; for
84 example, *Tumulitermes pastinator* mounds appear to be largely inactive and still a high
85 fraction of termite-derived CH₄ can be oxidised in soil beneath mounds, due to facilitation
86 of CH₄ transport within the mound [7]. It remains unclear whether differences in
87 methanotroph community abundance or composition account for these activity
88 differences.

89 In this work, we aimed to resolve these discrepancies by conducting a comprehensive
90 analysis of the composition and kinetics of the methanotroph communities within termite
91 mounds of Australian termite species. Three mound-building termite species were
92 selected, the wood-feeding *Microcerotermes nervosus* (Mn), soil-interface-feeding
93 *Macrognathotermes sunteri* (Ms), and grass-feeding *Tumulitermes pastinator* (Tp), which
94 represent the three main feeding groups present in Australia [17]. Mounds of these
95 species were previously confirmed to oxidise a high fraction of termite-produced CH₄ [7].
96 We used the *pmoA* gene, encoding a subunit of the particulate methane monooxygenase
97 present in most methanotrophs [18], as a molecular marker to study the abundance,
98 diversity, and composition of the methanotrophs within 17 mounds and a subset of
99 adjoining soils. In parallel, we performed *in situ* studies using gas push-pull tests (GPPTs)
100 to derive the kinetic parameters of CH₄ oxidation. We demonstrate that methanotrophic
101 communities in the core and periphery of termite mounds are compositionally and
102 kinetically distinct from those of surrounding soil, and primarily comprise methanotrophs
103 affiliated with the Upland Soil Cluster α (USC α) with an apparent medium affinity for CH₄.

104 **Materials and Methods**

105 **Field sites and sampling**

106 Field tests and sampling were performed in April and May 2016 in a coastal savanna
107 woodland on the campus of Charles Darwin University in Darwin, Northern Territory,
108 Australia (12.370° S, 130.867° E). The site is described in detail in Nauer et al. [7]. For
109 this study, 29 mounds were first subject to *in situ* methane kinetic measurements using
110 gas push-pull tests (described below). For further investigations following field
111 measurements, we selected 17 termite mounds of an appropriate size for processing in
112 the laboratory (initially 18, but one was damaged during transport and had to be
113 discarded). These mounds were first excavated but kept intact to measure internal
114 structure, volume, densities, and porosities as previously described [19]. They were then
115 deconstructed to (i) sample termites for species identification, (ii) collect mound material
116 for gravimetric water content measurements, and (iii) collect mound material for molecular
117 analyses of methanotrophic community. For species determination, soldiers were
118 individually picked and stored in pure ethanol for species confirmation as previously
119 described [19]. For gravimetric water content measurements, approximately 200 g of
120 mound material from both core and periphery locations were subsampled and oven dried
121 at 105 °C for >72 hours; subsamples were measured before and after drying and the
122 water content calculated based on mass loss. Subsamples for physicochemical
123 parameters were oven-dried at 60 °C for 72 h, carefully homogenised into a composite
124 sample for each termite species and location, and sent to an external laboratory for
125 analyses according to standard protocols (CSBP laboratories, Bibra Lake WA, Australia).
126 For community analysis, mound and soil material was collected under sterile conditions
127 using bleach- and heat-sterilised spatulas, and immediately stored in autoclaved 2 mL
128 centrifuge tubes at -20 °C. For each sampling location (mound core and periphery, soil
129 beneath and surrounding the mound), we collected triplicates of pooled materials deriving
130 from three different spots. Mound cores were sampled from within 20 to 30 cm from the
131 approximate centroid of mound, whereas mound periphery was collected from the outer
132 5 to 10 cm of the mound. For a subset of the investigated mounds, soil was collected from

133 beneath the mound immediately after mound excavation, and from the surrounding soil
134 within a 1-2 m radius from the mound.

135 **Genomic DNA isolation and *pmoA* gene amplification**

136 Each individual sample of mound material and soil was homogenised. DNA was extracted
137 from 0.25 to 0.5 grams of each sample using the PowerLyzer PowerSoil DNA Isolation
138 Kit (Qiagen, US), according to the manufacturer instructions. The purity and integrity of
139 the DNA extracts was verified by spectrophotometry (NanoDrop ND-1000
140 spectrophotometer, Nanodrop Technologies Inc., US) and PCR amplification of 16S
141 rRNA genes. Good yields of high-quality, amplifiable genomic DNA were obtained from
142 all 48 samples. Amplicons of the *pmoA* gene were also obtained from all samples using
143 previously described degenerate primers (A189f 5'-GGNGACTGGGACTTCTGG-3', and
144 mb661 5'-CCGGMGCAACGTCYTTACC-3') [20, 21] and cycling conditions [22].
145 Amplification reaction mixtures (25-50 μ L final volume) were prepared using 1 μ l of DNA
146 extract as template, 1 \times PCR buffer, 0.2 mM of each primer, 0.25 mM deoxynucleoside
147 triphosphates (dNTPs), and 0.025 U μ l⁻¹ of Taq polymerase (Takara Biotechnology Ltd.,
148 Japan). Different dilutions (undiluted to 1:100 in PCR-grade water) of DNA extracts were
149 used as template during amplification, and the dilution resulting in the highest yield and
150 quality of PCR product was used for further analyses.

151 **Quantitative PCR assays**

152 Quantitative PCR assays were used used to estimate the abundance of the total bacterial
153 community and methanotroph community. Total bacterial abundance was estimated by
154 amplifying the 16S rRNA gene using degenerate primers (515FB 5'-
155 GTGYCAGCMGCCGCGGTAA-3' and 806RB 5'-GGACTACNVGGGTWTCTAAT-3') and
156 cycling conditions as previously described [23–25]. Methanotroph abundance was
157 estimated by amplifying the *pmoA* gene using previously described degenerate primers
158 (A189f 5'-GGNGACTGGGACTTCTGG-3', and mb661 5'-CCGGMGCAACGTCYTTACC-
159 3') [20, 21] and cycling conditions [22]. Gene copy numbers were determined using a
160 LightCycler 480 real-time PCR system (Roche, Basel, CH). Individual reactions contained
161 1 \times PowerUp SYBR Green Master Mix (Thermo Fisher Scientific), 400 μ M of each primer,

162 and 1 μ l of diluted environmental DNA mixed to a final volume of 20 μ l. Thermal profiles
163 were adapted from those used for previous PCRs and included an acquisition step of 85
164 °C for 30 s at the end of each amplification cycle. Melting curve analysis was performed
165 as follows: 95 °C for 15 s, 60 °C for 60 s, 95 °C for 30 s, 60 °C for 15 s. For each assay
166 (96-well plate), duplicate serial dilutions of quantified DNA extract from *Methylosinus*
167 *trichosporium* were used for calibration curves to quantify 16 rRNA genes or *pmoA* genes.
168 Each sample was analyzed in triplicate, and a total of three assays were required for each
169 gene to include all the samples. Amplification efficiencies calculated from the slopes of
170 calibration curves were >70% and R^2 values were >0.98.

171 **Methanotroph community analysis**

172 The structure of the methanotroph community within each sample was inferred from
173 amplicon sequencing of community *pmoA* genes. DNA extracts of all samples were sent
174 to the Australian Genome Research Facility (AGRF; Brisbane, QLD) for preparation of
175 *pmoA* gene amplicon libraries using the above primer sets (A189f and mb661) and
176 thermal conditions. Subsequent amplicon sequencing was performed on a MiSeq DNA-
177 sequencing platform using a 600-cycle MiSeq Reagent Kit v3 (Illumina, San Diego, CA).
178 Sequencing yielded 5,594,739 paired end sequences, of which 3,078,335 passed quality
179 checks and data processing, and were used for subsequent analyses. Sequence read-
180 counts spanned three orders of magnitude (10^5 to 10^2), with 54% of the samples
181 exhibiting read counts above the average read-count value (>65K) and most mound
182 periphery samples having read-counts below 10K. Six samples with read-counts below
183 1K and were excluded from subsequent analyses. Sequencing data was processed
184 according to our previously published pipeline [26], with minor modifications. Briefly,
185 reads were 3'-trimmed to remove ambiguous or low-quality endings, then merged and
186 primer-site trimmed. Quality filters included an amplicon-size selection (471 nt) and the
187 removal of amplicons containing stop codons (e.g., TAA, TAG, TGA). Sequences were
188 also checked for correct open reading frames (ORF) using the FrameBot tool
189 (<http://fungene.cme.msu.edu/FunGenePipeline/framebot/form.spr>). The centroid
190 clustering method [27] identified 25 Operational Taxonomic Units (OTUs) that shared
191 86% nucleotide sequence similarity [28] with sequences from a curated *pmoA* gene

192 database derived from Dumont et al., 2014 [29]. Phylogenetic distances of the assigned
193 OTUs in relation to reference *pmoA* sequences were assessed as previously described
194 [26]. The phylogenetic tree of protein-derived *pmoA* sequences was constructed using
195 the maximum-likelihood method and the LG empirical amino acid substitution model,
196 which showed the lowest Akaike information criterion (AIC) during substitution model
197 testing, and was bootstrapped using 100 bootstrap replicates. All sequences affiliated
198 with methanotrophs and no *pxmA* or *amoA* sequences were detected.

199 **Phylogenetic and diversity analyses**

200 Alpha and beta diversity calculations, as well as read count normalization of the *pmoA*
201 sequences, were performed with the package phyloseq v1.12.2 [30] from the open source
202 software Bioconductor. To account for differences in numbers of reads between samples,
203 we rarefied OTU counts to an even sampling depth of 1,611 read counts. Chao1,
204 Shannon, and Inverse Simpson indices were computed to assess the alpha diversity of
205 MOB communities. Beta diversity of methanotroph communities was measured using the
206 phylogenetic metric Unifrac weighted by the relative abundance of individual OTUs
207 (Lozupone and Knight, 2005). Differences were visualised using non-parametric multi-
208 dimensional scaling ordinations (nMDS). To determine whether the observed between-
209 group distances were statistically significant, we performed permutational multivariate
210 analysis of variance (PERMANOVA) with the software PRIMER-E v7 (PRIMER-E Ltd.,
211 Plymouth, United Kingdom). Negative binomial models were performed on the non-
212 rarefied OTU dataset to assess the differential abundance of bacterial OTUs between
213 sample groups, and the false discovery rate approach was used to account for multiple
214 testing.

215 **Gas push-pull tests**

216 The gas push-pull test was used to estimate *in situ* activity coefficients as described
217 previously [19, 31]. Michaelis-Menten parameters estimated from *in situ* methods are
218 integrated measures across a large mass of substrate and are thus better suited to
219 characterise the kinetic potential of whole microbial communities in heterogeneous
220 systems than laboratory microcosms, which suffer from inevitable sampling bias [32]. In

221 brief, a gas mixture containing laboratory air, ~900 $\mu\text{L L}^{-1}$ of CH_4 , and ~0.1 L L^{-1} argon
222 (Ar) was injected at a rate of ~0.5 L min^{-1} into the lower center of the termite mounds and
223 then immediately extracted from the same location at the same flow rate. During
224 extraction, the injected gas mixture was gradually diluted with termite-mound air down to
225 background levels; the tracer Ar accounted for this dilution due to its similar transport
226 behavior to CH_4 . A timeseries of CH_4 and Ar concentrations was collected during the 24
227 min injection phase, and the 36 min extraction phase. Concentrations of CH_4 were
228 measured quasi-continuously (frequency of 1 Hz) using a field-portable spectrometer
229 (Fast Greenhouse Gas Analyser Los Gatos Research, Mountain View, CA). For Ar,
230 discrete samples were collected at fixed intervals during injection ($n = 3$) and extraction
231 ($n = 10-12$), as well as prior to injection to determine background levels. Argon
232 concentrations were analysed on a customised gas chromatography system (SRI 8610,
233 SRI Instruments, Torrance, CA) with an external thermal conductivity detector (TCD; VICI
234 Valco Instruments Co., Houston, TX). To improve separation of Ar, oxygen was removed
235 from the sample-gas stream prior to separation with a manually packed Pd-Al catalyst
236 column [19, 33].

237 **Kinetic analysis**

238 First-order rate coefficients of CH_4 oxidation (activity coefficient k) were estimated from
239 GPPTs via the slope of the logarithm of relative CH_4 vs Ar concentrations, plotted against
240 a transformed reaction time, according to the plug-flow reactor model for simplified GPPT
241 analysis [34]. This data also allowed the calculation of reaction rates at different CH_4
242 concentrations from segments of the extraction time-series, and thus the estimation of
243 Michaelis-Menten parameters [35]. The running average of CH_4 concentrations C_{CH_4} over
244 three consecutive extraction samples was multiplied with the corresponding activity (k)
245 from the logarithmic plot to calculate an individual reaction rate R_{ox} for each segment. The
246 Michaelis-Menten parameters K_m and V_{max} were then estimated for each individual GPPT,
247 and for all combined pairs of concentrations and reaction rates, by fitting the Michaelis-
248 Menten model $R_{\text{ox}} = V_{\text{max}} * C_{\text{CH}_4} / (K_m + C_{\text{CH}_4})$ to the data using the non-linear regression
249 routine `nls()` in R [36]. The AIC was calculated and compared with a linear regression
250 model of R_{ox} vs C_{CH_4} ; if the AIC of the linear model was lower, no Michaelis-Menten

251 parameters were reported. Cell-specific activities and rates were calculated from reaction
252 rates based on total mound dry mass, divided by *pmoA* copy numbers and assuming two
253 gene copies of *pmoA* per cell. Correlations between kinetic parameters (k , K_m , V_{max}), gene
254 abundance (*pmoA* and 16S), and physical mound parameters (mound porosities, volume,
255 water content) were tested for significance using linear regression, after transformations
256 (sqrt for kinetic parameters, log for gene abundances) and removal of outliers as indicated
257 by diagnostic plots (qq- and Cook's distance).

258 **Results and Discussion**

259 **Methanotrophic bacteria are in low abundance in termite mounds and associated
260 soils**

261 Quantitative PCR was used to estimate the abundance of the methanotroph community
262 (*pmoA* copy number) and total bacterial community (16S gene copy number) in each
263 mound and soil sample. Bacterial abundance was consistently high (av. 2.7×10^{10} 16S
264 copy numbers per gram of dry soil; range 2.5×10^8 to 3.4×10^{11}) and did not significantly
265 differ between sample locations (**Fig. 1b & Fig. S1**); an earlier study found higher
266 microbial biomass in the mound compared to soil [37], but this may reflect different
267 methodologies applied to each substrate. In contrast, *pmoA* copy number was relatively
268 low across the samples (av. 1.5×10^6 copies per gram of dry sample material; range: 2.0×10^4 to 1.8×10^7) and just 0.0076% that of 16S copy number (range: 0.00018% to
269 0.048%) (**Figure 1a**). Such values are comparable to those previously reported for the
270 abundance of *pmoA* genes in upland soils that mediate atmospheric CH₄ oxidation (~ 10^6
271 copy number, ~0.01% relative abundance [38]).

273 Some differences in methanotroph abundance were observed between sample locations
274 and termite species. Overall, *pmoA* copy number was 3.5-fold higher in mound core and
275 1.5-fold higher in soil beneath than in surrounding soil, though differences were below the
276 threshold of significance (**Fig. S1**). In contrast, *pmoA* copy numbers were significantly
277 lower in mound periphery samples of all species ($p = 0.028$) (**Fig. S1**) and in mound
278 samples of *T. pastinator* compared to the other two species tested ($p = 0.028$) (**Fig. S2**);
279 the latter observation is in line with the finding that CH₄ oxidation occurs at low rates in *T.*

280 *pastinator* mound material [7]. Consistently, *pmoA* copy numbers were significantly
281 positively correlated with the porosity of the mound material, with periphery samples
282 showing a stronger dependence ($R^2 = 0.49$, $p = 0.0051$) than core ($R^2 = 0.26$, $p = 0.035$);
283 this suggests that denser mound material, as found in mound periphery and *T. pastinator*
284 mounds, limits methanotroph abundance [19]. These differences may also reflect the
285 relatively harsh conditions in the mound periphery, with its strong fluctuations of
286 temperature and water content, compared to the core with termite-engineered
287 homeostasis [39, 40]. Other physical parameters did not correlate with *pmoA* or 16S copy
288 numbers.

289 **Termite mound methanotroph communities are compositionally distinct from
290 those of associated soils**

291 The composition and diversity of the methanotroph community in each sample was
292 inferred through amplicon sequencing of the *pmoA* gene. Across the samples, 25 OTUs
293 were detected (**Figure 2**). Observed and estimated richness of these OTUs was higher
294 in soil samples compared to mound samples (av. Chao1 of 9.0 for mound core, 5.9 for
295 mound periphery, 12.3 for soil samples; $p < 0.001$) (**Figure 1c**); however, these
296 differences were driven primarily by rare OTUs in soil samples, with Shannon and inverse
297 Simpson indices similar between samples (**Figure S3**). Beta diversity of the samples was
298 analysed by weighted Unifrac and visualised on an nMDS ordination plot (**Figure 3a**).
299 PERMANOVA analysis confirmed communities significantly differed between sample
300 locations ($p = 0.001$) and termite species ($p = 0.022$). With respect to sample location,
301 communities within mound core and periphery samples were similar and were
302 compositionally distinct from soil communities; in addition, methanotroph communities in
303 soils beneath mounds were more similar to those within mounds than those in soils
304 surrounding mounds. This confirms previous inferences that mound and soil communities
305 are different and shaped by termite activity [14]. In addition, core and peripheral mound
306 communities significantly clustered by termite species, while soil samples did not; mound
307 communities of *M. nervosus* and *T. pastinator* were more closely related than those of *M.*
308 *sunteri* (**Figure 3a**).

309 The 25 OTUs detected were visualised on a phylogenetic tree against reference
310 sequences from a curated *pmoA* gene database [29]. Phylogenetic analysis indicates that
311 all OTUs were affiliated with proteobacterial methanotroph sequences (**Figure 2**). Across
312 all samples, over 80% of the sequences were affiliated with USC α , a recently cultivated
313 lineage of alphaproteobacterial methanotrophs known to mediate atmospheric CH₄
314 oxidation [41, 42] (**Figure 2 & Figure 3b**). The second most dominant taxonomic groups
315 were affiliated with the alphaproteobacterial lineages *Methylocystis* in mound samples
316 (<10% relative abundance) and the gammaproteobacterial lineage TUSC in soil samples
317 (<10% relative abundance). There was a large proportion of shared taxa across the
318 samples, with the three most abundant OTUs (USC α -affiliated) present in all samples,
319 regardless of type (mound vs soil), location and termite species (**Figure 3b**). However,
320 differential abundance analysis supported the observed differences between sample type
321 and termite species observed by Unifrac analysis (**Figure 3a**). Overall, USC α and
322 *Methylocystis* OTUs were more abundant in mound core, mound periphery, and soils
323 beneath, whereas TUSC OTUs were more abundant in surrounding soils. Significant
324 differential abundance was also observed for certain OTUs between termite species
325 (**Figure 3b**).

326 It should be noted that community composition of the mounds from the three Australian
327 termite species strikingly differs from those of the African fungus-growing termite
328 *Macrotermes falciger* [14]. These African mounds were dominated by the Jasper Ridge 3
329 cluster (JR3), a gammaproteobacterial methanotroph lineage closely related to USC γ ,
330 which was not detected in the Australian mounds (**Figure 2**). These differences may
331 reflect the distinct habitat specificity of USC γ and USC α methanotrophs. USC α often
332 occurs in acidic to neutral upland soils ([43], reviewed in [18]), which match the pH values
333 of 5 measured in the mounds of this study (**Table S1**). In contrast, USC γ and associates
334 lineages are commonly found in upland soils of neutral to basic pH [44, 45], which
335 corresponds well to pH values of 7 to 8 in *Macrotermes falciger* mounds [14].

336 **Methanotroph communities are kinetically adapted to elevated CH₄ concentrations**

337 We determined the kinetics of CH₄ oxidation in the mounds by performing *in situ* GPPTs.
338 Methane oxidation rate was high across the 29 mounds from all three species

339 investigated (**Figure 4a**). The relationship between CH_4 concentration and reaction rate
340 best fitted a Michaelis-Menten model for 18 mounds and a linear model for 11 mounds
341 based on AIC values (**Figure 4a**). For the former group of mounds, apparent Michaelis-
342 Menten coefficients (K_m , V_{max}) were calculated. Estimated K_m values for the 18 mounds
343 ranged from 0.32 to 47 $\mu\text{mol (L air)}^{-1}$, and V_{max} from 8.4 to 280 $\mu\text{mol (L air)}^{-1} \text{ h}^{-1}$. These
344 parameters did not significantly differ between termite species. The overall mean values
345 for K_m and V_{max} were $17.5 \pm 3.5 \mu\text{mol (L air)}^{-1}$ and $78.3 \pm 17 \mu\text{mol (L air)}^{-1} \text{ h}^{-1}$, respectively
346 (standard error of the mean); such values were close to the optimal parameters when
347 fitting a Michaelis-Menten model to combined GPPT data (excluding mounds with linear
348 behavior): $K_m = 13.2 \pm 3.5 \mu\text{mol (L air)}^{-1}$ and $V_{max} = 55.4 \pm 8.5 \mu\text{mol (L air)}^{-1} \text{ h}^{-1}$ (**Figure**
349 **4a and 4b**). Thus, the methanotroph communities within termite mounds have an
350 apparent medium (μM) affinity for CH_4 . The apparent K_m is approximately one to two
351 orders of magnitude higher than high-affinity (nM) uptake observed in upland soils [46–
352 48], but one to two orders of magnitude lower than the low-affinity (mM) uptake measured
353 in landfill-cover soils [49]. Similar Michaelis-Menten values were estimated from GPPTs
354 in the vadose zone above a contaminated aquifer (~ 1 to $40 \mu\text{L L}^{-1}$), which featured CH_4
355 concentrations in a similar range to termite mounds [35].

356 It is noteworthy that 11 mounds showed an apparent linear increase of reaction rates with
357 substrate concentrations (**Figure 4a**). This could indicate that V_{max} has not been reached
358 during GPPTs with a maximum injected CH_4 concentration of $\sim 900 \mu\text{L L}^{-1}$ ($\sim 40 \mu\text{M}$);
359 indeed, the injection concentration is in the range of our highest K_m , thus the capacity of
360 some mounds to oxidise CH_4 can be substantially higher. A linear increase could also
361 indicate a shift in kinetics during the course of the GPPT. It is in the nature of the GPPT
362 that different areas of the mound are exposed to different concentration ranges,
363 depending on their distance to the gas injection/extraction point [34]. Hence, gas
364 extracted at different times may have had a “history” of exposure to methanotroph
365 communities with different kinetics. It is even conceivable that the 1 h long exposure to
366 high injection concentrations around the injection/extraction point triggered the
367 upregulation of a low-affinity methane monooxygenase isozyme, such as those reported
368 in *Methylocystis* sp. SC2 [50].

369 For the 17 selected mounds investigated in more detail, we analysed how the kinetics
370 and abundance of the methanotroph communities were correlated. While a range of
371 positive correlations were observed, the most robustly supported was the relationship
372 between the first-order activity coefficient k and termite mound core *pmoA* copy number
373 ($R^2 = 0.44$, $p = 0.007$) (**Figure 4c**). In contrast, correlations with *pmoA* copy number in
374 periphery and soils were not significant. These observations are in line with previous
375 inferences that mound cores are primarily responsible for CH_4 oxidation in *M. nervosus*
376 and *M. sunteri* mounds [7]. On this basis, cell-specific CH_4 reaction rates calculated based
377 on methanotroph abundance of the mound core ranged from 1.8×10^{-17} to 1.3×10^{-14} mol
378 CH_4 cell $^{-1}$ h $^{-1}$, one to two orders of magnitude higher than observed in upland soils [38].
379 Though differences between species were not significant, highest cell-specific rates were
380 calculated for *T. pastinator*, with some values close to a value determined from a landfill-
381 cover biofilter [51]. This would imply that these methanotroph communities operate close
382 to their maximum potential of CH_4 oxidation. However, it is likely that values for *T.*
383 *pastinator* are an overestimate given previous studies indicate that most CH_4 for this species
384 but not the two others tested, core *pmoA* numbers underestimate the active methanotroph
385 community involved in mitigating termite CH_4 emissions.

387 **Conclusions and perspectives**

388 Overall, our results imply that local environmental concentrations of CH_4 shape the
389 composition and kinetics of the methanotroph community. Elevated CH_4 production from
390 termites appears to have selected for a specialised medium-affinity methanotroph
391 community within mounds. The community analysis shows that the methanotroph
392 communities within termite mounds are related to, and likely derived from, those of
393 adjoining soils. However, elevated CH_4 availability and termite activity have facilitated
394 selection for USCa and *Methylocystis* OTUs, together with exclusion of TUSC OTUs,
395 compared to adjoining soil. These methanotroph communities, with high cell-specific
396 reaction rates and medium affinities for CH_4 , are thus ideally kinetically adapted to grow
397 on termite-derived CH_4 and in turn reduce atmospheric emissions of this greenhouse gas.
398 Concordant findings were made across three different species, with the strongest

399 relationships between methanotroph abundance and methane oxidation parameters
400 observed for *M. nervosus* and *M. sunteri* mounds.

401 However, the apparent kinetic parameters of methane oxidation in termite mounds are
402 atypical of the dominant groups of methanotrophs present. It is probable that USC α
403 mediates most methane oxidation in mounds, given their abundance and prevalence in
404 the mound core methanotroph communities, as well as the high cell-specific rates of
405 methane oxidation measured. However, USC α are typically high-affinity methanotrophs
406 associated with the oxidation of CH₄ at atmospheric concentrations in upland soils. There
407 are several possible explanations for this discrepancy. Firstly, while members of USC α in
408 soil and mound share the same methane monooxygenase, the selective pressure of
409 enhanced methane availability may have caused mound inhabitants to evolve faster-
410 acting, lower-affinity variants. An alternative explanation is community heterogeneity. Any
411 apparent Michaelis-Menten parameter estimates from environmental samples are ‘bulk’
412 values integrating across the whole microbial community and thus a vast array of
413 potentially different enzymes. Indeed, the observed *in situ* kinetics are also compatible
414 with the coexistence of slow-acting, high-affinity USC α methanotrophs alongside faster-
415 acting, low-affinity other groups. While CH₄ concentrations in mounds are elevated
416 compared to the atmosphere [7, 52], they are generally within an accessible range for
417 high-affinity methanotrophs (2 – 100 ppmv). *Methylocystis*-like OTUs, as the second most
418 abundant group, are likely to be particularly competitive at high CH₄ concentrations.
419 Members of this group encode kinetically distinct methane monooxygenase isozymes [50]
420 and have been identified in other soils with elevated methane concentrations [22]. They
421 would therefore have a competitive advantage in termite mounds where CH₄ availability
422 is elevated and exhibits considerable temporal and spatial variation.

423 However, despite elevated substrate availability, methanotrophs remain minor members
424 of microbial communities in termite mounds. While they are moderately enriched in
425 mound core than adjoining soil overall, they are actually diminished relative to soil in both
426 the mound core of *T. pastinator* and the periphery of all three species. The observed
427 strong correlation of methanotroph abundance with the porosity of the mound material for
428 all species strengthens the case for habitat porosity as a crucial factor in regulating the

429 methanotrophic community, likely by regulating local CH₄ availability through diffusion.
430 Another factor driving low methanotroph abundance could be the accumulation of
431 ammonia, which is known to be produced in high levels by termites [53]; it is known that
432 ammonia competitively inhibits methane monooxygenase activity [54, 55] and ammonia
433 levels are major environmental factors regulating methanotroph community in soils [56,
434 57]. However, while we detected high ammonia concentrations in some mounds (**Table**
435 **S1**), this did not correlate with interspecies differences in methanotroph abundance. It is
436 also possible that the methanotrophs are limited by other factors, such as the
437 micronutrients required for methane monooxygenase activity. Ultimately, given
438 methanotrophs remain minor members of the termite mound community, they are only
439 able to mitigate a proportion of the large amounts of methane produced by mound-
440 dwelling termites.

441 **Acknowledgements**

442 We thank Thanavit Jirapanjawat, Lindsay Hutley and Matthew Northwood for technical
443 and logistical assistance, and Andreas Brune for an inspiring correspondence. This work
444 was supported by Australian Research Council grants (DP120101735 and LP100100073
445 awarded to S.K.A.), Swiss National Science Foundation Early Postdoc Mobility
446 Fellowships (P2EZP3_178421 awarded to E.C.; P2EZP3_155596 awarded to P.A.N.), an
447 ARC DECRA Fellowship (DE170100310 awarded to C.G.), the Terrestrial Ecosystem
448 Research Network (TERN) OzFlux, and the TERN Australian SuperSite Network.

449 Author contributions: P.A.N., E.C., S.K.A., and C.G. designed the study. E.C. and P.A.N.
450 performed field and laboratory work. E.C., P.A.N., and C.G. analyzed data. C.G., E.C.,
451 P.A.N., and S.K.A. wrote and edited the paper.

452 **References**

- 453 1. Brune A. Methanogenesis in the digestive tracts of insects. *Handbook of*
454 *hydrocarbon and lipid microbiology*. 2010. Springer, pp 707–728.
- 455 2. Zimmerman PR, Greenberg JP, Wandiga SO, Crutzen PJ. Termites: a potentially
456 large source of atmospheric methane, carbon dioxide, and molecular hydrogen.
457 *Science (80-)* 1982; **218**: 563–565.
- 458 3. Rasmussen RA, Khalil MAK. Global production of methane by termites. *Nature*

459 1983; **301**: 700.

460 4. Sugimoto A, Inoue T, Tayasu I, Miller L, Takeichi S, Abe T. Methane and
461 hydrogen production in a termite-symbiont system. *Ecol Res* 1998; **13**: 241–257.

462 5. Brauman A, Kane MD, Labat M, Breznak JA. Genesis of acetate and methane by
463 gut bacteria of nutritionally diverse termites. *Science (80-)* 1992; **257**: 1384–
464 1387.

465 6. Kirschke S, Bousquet P, Ciais P, Saunois M, Canadell JG, Dlugokencky EJ, et al.
466 Three decades of global methane sources and sinks. *Nat Geosci* 2013; **6**: 813–
467 823.

468 7. Nauer PA, Hutley LB, Arndt SK. Termite mounds mitigate half of termite methane
469 emissions. *Proc Natl Acad Sci* 2018; **115**: 13306–13311.

470 8. Hanson RS, Hanson TE. Methanotrophic bacteria. *Microbiol Rev* 1996; **60**: 439–
471 471.

472 9. Reuß J, Rachel R, Kämpfer P, Rabenstein A, Küver J, Dröge S, et al. Isolation of
473 methanotrophic bacteria from termite gut. *Microbiol Res* 2015; **179**: 29–37.

474 10. Pester M, Tholen A, Friedrich MW, Brune A. Methane oxidation in termite
475 hindguts: absence of evidence and evidence of absence. *Appl Environ Microbiol*
476 2007; **73**: 2024–2028.

477 11. Dunfield PF. The Soil Methane Sink. In: Reay D, Hewitt K, Smith K, Grace J
478 (eds). *Greenhouse Gas Sinks*. 2007. CABI, Wallingford, pp 152–170.

479 12. Bignell DE, Eggleton P, Nunes L, Thomas KL. Termites as mediators of carbon
480 fluxes in tropical forest: budgets for carbon dioxide and methane emissions. *For
481 insects* 1997; 109–134.

482 13. Jamali H, Livesley SJ, Grover SP, Dawes TZ, Hutley LB, Cook GD, et al. The
483 importance of termites to the CH₄ balance of a tropical savanna woodland of
484 northern Australia. *Ecosystems* 2011; **14**: 698–709.

485 14. Ho A, Erens H, Mujinya BB, Boeckx P, Baert G, Schneider B, et al. Termites
486 facilitate methane oxidation and shape the methanotrophic community. *Appl
487 Environ Microbiol* 2013; **79**: 7234–7240.

488 15. Noirot C, Darlington JPEC. Termite nests: architecture, regulation and defence.
489 *Termites: evolution, sociality, symbioses, ecology*. 2000. Springer, pp 121–139.

490 16. Korb J. Termite mound architecture, from function to construction. *Biology of
491 termites: a modern synthesis*. 2010. Springer, pp 349–373.

492 17. Jones DT, Eggleton P. Global Biogeography of Termites: A Compilation of
493 Sources. In: Bignell DE, Roisin Y, Lo N (eds). *Biology of Termites: A Modern
494 Synthesis*. 2011. Springer, Dordrecht, pp 1–576.

495 18. Knief C. Diversity and habitat preferences of cultivated and uncultivated aerobic
496 methanotrophic bacteria evaluated based on *pmoA* as molecular marker. *Front
497 Microbiol* 2015; **6**: 1346.

498 19. Nauer PA, Chiri E, Souza D de, Hutley LB, Arndt SK. Rapid image-based field
499 methods improve the quantification of termite mound structures and greenhouse-

500 gas fluxes. *Biogeosciences* 2018; **15**: 3731–3742.

501 20. Holmes AJ, Costello A, Lidstrom ME, Murrell JC. Evidence that participate
502 methane monooxygenase and ammonia monooxygenase may be evolutionarily
503 related. *FEMS Microbiol Lett* 1995; **132**: 203–208.

504 21. Costello AM, Lidstrom ME. Molecular characterization of functional and
505 phylogenetic genes from natural populations of methanotrophs in lake sediments.
506 *Appl Environ Microbiol* 1999; **65**: 5066–5074.

507 22. Henneberger R, Chiri E, Bodelier PEL, Frenzel P, Lüke C, Schroth MH. Field-
508 scale tracking of active methane-oxidizing communities in a landfill cover soil
509 reveals spatial and seasonal variability. *Environ Microbiol* 2015; **17**: 1721–1737.

510 23. Caporaso JG, Lauber CL, Walters WA, Berg-Lyons D, Lozupone CA, Turnbaugh
511 PJ, et al. Global patterns of 16S rRNA diversity at a depth of millions of
512 sequences per sample. *Proc Natl Acad Sci* 2011; **108**: 4516–4522.

513 24. Parada AE, Needham DM, Fuhrman JA. Every base matters: assessing small
514 subunit rRNA primers for marine microbiomes with mock communities, time series
515 and global field samples. *Environ Microbiol* 2016; **18**: 1403–1414.

516 25. Apprill A, McNally S, Parsons R, Weber L. Minor revision to V4 region SSU rRNA
517 806R gene primer greatly increases detection of SAR11 bacterioplankton. *Aquat
518 Microb Ecol* 2015; **75**: 129–137.

519 26. Chiri E, Nauer PA, Rainer E-M, Zeyer J, Schroth MH. High temporal and spatial
520 variability of atmospheric-methane oxidation in Alpine glacier-forefield soils. *Appl
521 Environ Microbiol* 2017; **83**: e01139-17.

522 27. Edgar RC. Search and clustering orders of magnitude faster than BLAST.
523 *Bioinformatics* 2010; **26**: 2460–2461.

524 28. Wen X, Yang S, Liebner S. Evaluation and update of cutoff values for
525 methanotrophic pmoA gene sequences. *Arch Microbiol* 2016; **198**: 629–636.

526 29. Dumont MG, Lüke C, Deng Y, Frenzel P. Classification of pmoA amplicon
527 pyrosequences using BLAST and the lowest common ancestor method in
528 MEGAN. *Front Microbiol* 2014; **5**: 34.

529 30. McMurdie PJ, Holmes S. phyloseq: an R package for reproducible interactive
530 analysis and graphics of microbiome census data. *PLoS One* 2013; **8**: e61217.

531 31. Urmann K, Gonzalez-Gil G, Schroth MH, Hofer M, Zeyer J. New field method:
532 Gas push– pull test for the in-situ quantification of microbial activities in the
533 vadose zone. *Environ Sci Technol* 2005; **39**: 304–310.

534 32. Reim A, Lüke C, Krause S, Pratscher J, Frenzel P. One millimetre makes the
535 difference: high-resolution analysis of methane-oxidizing bacteria and their
536 specific activity at the oxic–anoxic interface in a flooded paddy soil. *ISME J* 2012;
537 **6**: 2128.

538 33. Raj SS, Sumangala RK, Lal KB, Panicker PK. Gas chromatographic analysis of
539 oxygen and argon at room temperature. *J Chromatogr Sci* 1996; **34**: 465–467.

540 34. Schroth MH, Istok JD. Models to determine first-order rate coefficients from

single-well push-pull tests. *Groundwater* 2006; **44**: 275–283.

35. Urmann K, Schroth MH, Noll M, Gonzalez-Gil G, Zeyer J. Assessment of microbial methane oxidation above a petroleum-contaminated aquifer using a combination of in situ techniques. *J Geophys Res Biogeosciences* 2008; **113**.

36. R Development Core Team. R: A Language and Environment for Statistical Computing. 2017. R Foundation for Statistical Computing, Vienna, Austria.

37. Holt JA. Microbial activity in the mounds of some Australian termites. *Appl Soil Ecol* 1998; **9**: 183–187.

38. Kolb S, Knief C, Dunfield PF, Conrad R. Abundance and activity of uncultured methanotrophic bacteria involved in the consumption of atmospheric methane in two forest soils. *Environ Microbiol* 2005; **7**: 1150–1161.

39. King H, Ocko S, Mahadevan L. Termite mounds harness diurnal temperature oscillations for ventilation. *Proc Natl Acad Sci* 2015; **112**: 11589–11593.

40. Bristow KL, Holt JA. Can termites create local energy sinks to regulate mound temperature? *J Therm Biol* 1987; **12**: 19–21.

41. Tveit AT, Hestnes AG, Robinson SL, Schintlmeister A, Dedysh SN, Jehmlich N, et al. Widespread soil bacterium that oxidizes atmospheric methane. *Proc Natl Acad Sci* 2019; 201817812.

42. Pratscher J, Vollmers J, Wiegand S, Dumont MG, Kaster A-K. Unravelling the identity, metabolic potential and global biogeography of the atmospheric methane-oxidizing Upland Soil Cluster α. *Environ Microbiol* 2018; **20**: 1016–1029.

43. Knief C, Lipski A, Dunfield PF. Diversity and activity of methanotrophic bacteria in different upland soils. *Appl Environ Microbiol* 2003; **69**: 6703–6714.

44. Chiri E, Nauer PA, Henneberger R, Zeyer J, Schroth MH. Soil–methane sink increases with soil age in forefields of Alpine glaciers. *Soil Biol Biochem* 2015; **84**: 83–95.

45. Angel R, Conrad R. In situ measurement of methane fluxes and analysis of transcribed particulate methane monooxygenase in desert soils. *Environ Microbiol* 2009; **11**: 2598–2610.

46. Bender M, Conrad R. Kinetics of CH₄ oxidation in oxic soils exposed to ambient air or high CH₄ mixing ratios. *FEMS Microbiol Lett* 1992; **101**: 261–270.

47. Nauer PA, Schroth MH. In situ quantification of atmospheric methane oxidation in near-surface soils. *Vadose Zo J* 2010; **9**: 1052–1062.

48. Judd CR, Koyama A, Simmons MP, Brewer P, von Fischer JC. Co-variation in methanotroph community composition and activity in three temperate grassland soils. *Soil Biol Biochem* 2016; **95**: 78–86.

49. Schroth MH, Eugster W, Gómez KE, Gonzalez-Gil G, Niklaus PA, Oester P. Above-and below-ground methane fluxes and methanotrophic activity in a landfill-cover soil. *Waste Manag* 2012; **32**: 879–889.

50. Baani M, Liesack W. Two isozymes of particulate methane monooxygenase with different methane oxidation kinetics are found in *Methylocystis* sp. strain SC2.

582 *Proc Natl Acad Sci* 2008; **105**: 10203–10208.

583 51. Gebert J, Stralis-Pavese N, Alawi M, Bodrossy L. Analysis of methanotrophic
584 communities in landfill biofilters using diagnostic microarray. *Environ Microbiol*
585 2008; **10**: 1175–1188.

586 52. Jamali H, Livesley SJ, Hutley LB, Fest B, Arndt SK. The relationships between
587 termite mound CH₄/CO₂ emissions and internal concentration ratios are species
588 specific. *Biogeosciences* 2013; **10**: 2229–2240.

589 53. Rong JI, Brune A. Nitrogen mineralization, ammonia accumulation, and emission
590 of gaseous NH₃ by soil-feeding termites. *Biogeochemistry* 2006; **78**: 267–283.

591 54. Schnell S, King GM. Mechanistic analysis of ammonium inhibition of atmospheric
592 methane consumption in forest soils. *Appl Environ Microbiol* 1994; **60**: 3514–
593 3521.

594 55. Carlsen HN, Joergensen L, Degn H. Inhibition by ammonia of methane utilization
595 in *Methylococcus capsulatus* (Bath). *Appl Microbiol Biotechnol* 1991; **35**: 124–
596 127.

597 56. Bodelier PLE, Laanbroek HJ. Nitrogen as a regulatory factor of methane oxidation
598 in soils and sediments. *Fems Microbiol Ecol* 2004; **47**: 265–277.

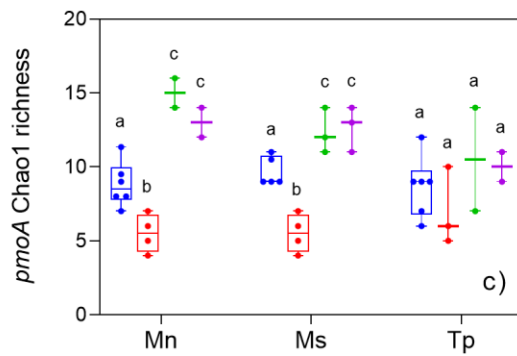
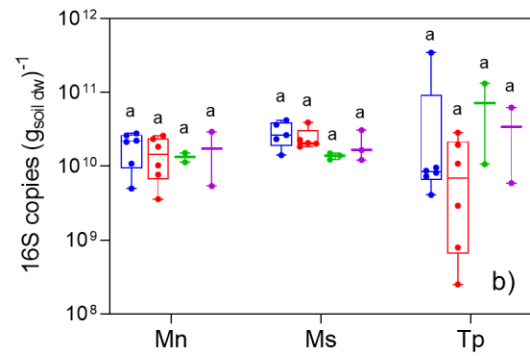
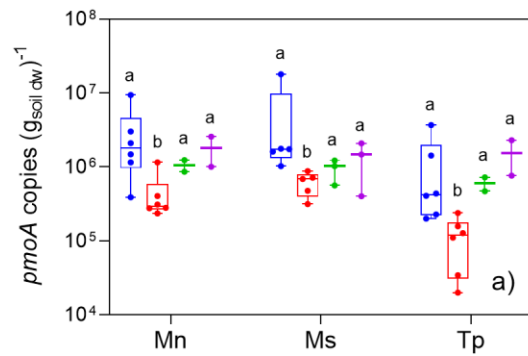
599 57. Veraart AJ, Steenbergh AK, Ho A, Kim SY, Bodelier PLE. Beyond nitrogen: The
600 importance of phosphorus for CH₄ oxidation in soils and sediments.
601 *Geoderma* 2015; **259–260**.

602

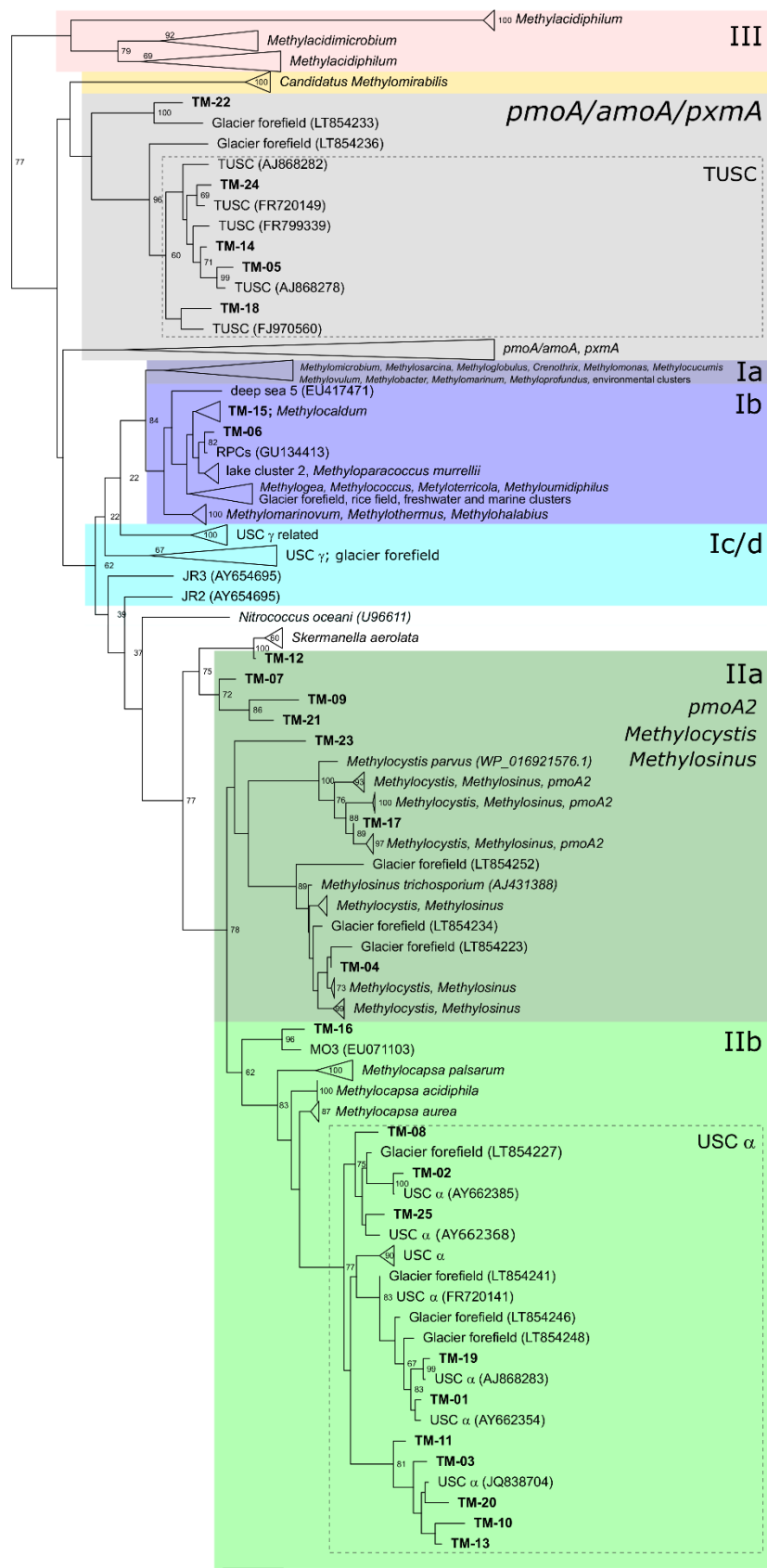
603

604 **Figures**

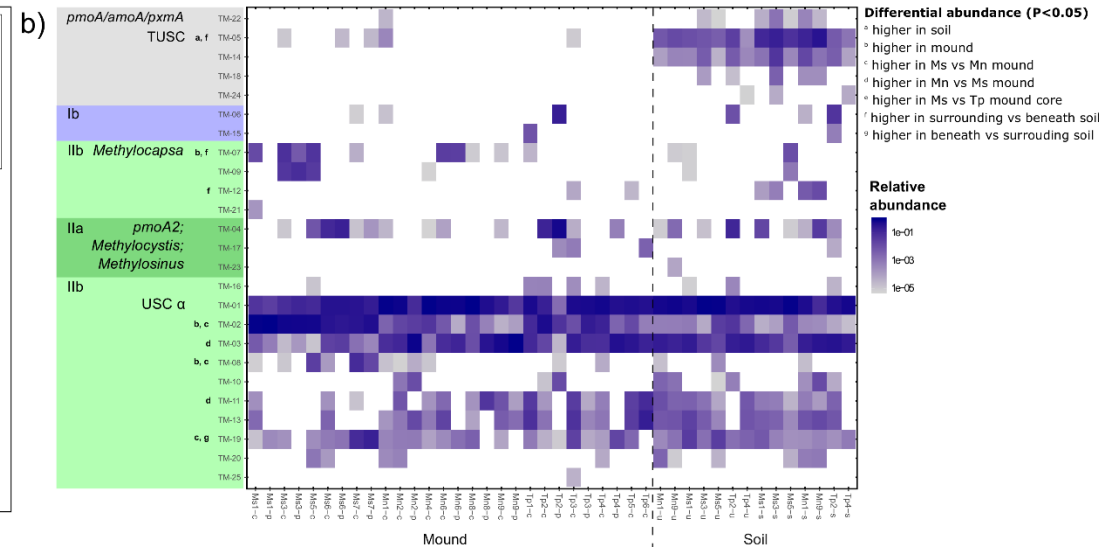
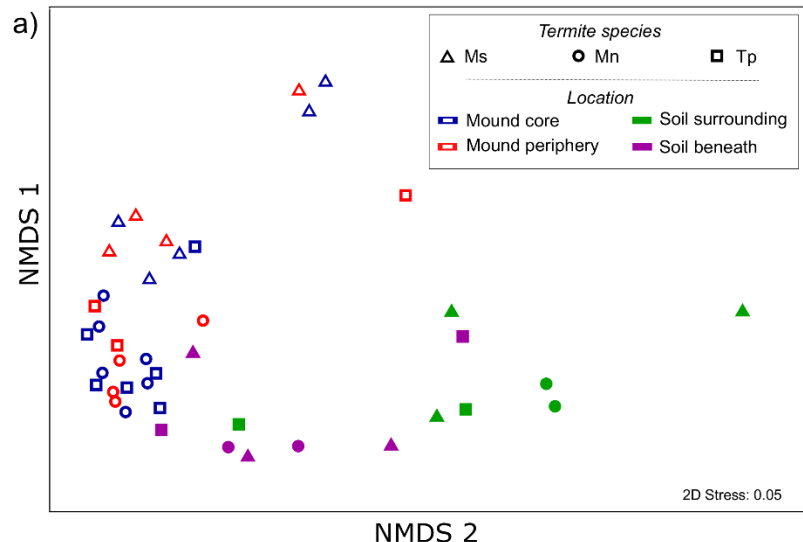
605 **Figure 1.** Abundance and richness of methane-oxidising bacteria (methanotrophs) in the
606 mounds and adjoining soils. a) Abundance of the methanotroph community, based on
607 copy number of the *pmoA* gene encoding the particulate methane monooxygenase 27
608 kDa subunit gene as determined by qPCR. b) Abundance of the total bacterial and
609 archaeal community, based on copy number of the universal 16S rRNA gene (V4 region)
610 as determined by qPCR. c) Estimated richness of the methanotroph community, based
611 on Chao1 index of the *pmoA* gene as determined by amplicon sequencing. Mound
612 samples (core and periphery) and adjoining soil samples (surrounding and beneath) were
613 tested from mounds of three different termite species (*Microcerotermes nervosus*, Mn;
614 *Macrognathotermes sunteri*, Ms; *Tumulitermes pastinator*, Tp). The box plots show
615 minimum, lower quartile, median, upper quartile, and maximum values, with all individual
616 values shown. Different letters denote significant differences between sample groups (p
617 < 0.05 , Wilcoxon signed-rank test).



619 **Figure 2.** Maximum-likelihood tree showing the phylogenetic affiliation of the protein-
620 derived *pmoA* gene sequences of 25 Operational Taxonomic Units (OTUs), in relation to
621 uncultivated methanotrophic clusters and methanotroph isolates. The tree was built using
622 the LG empirical amino acid substitution model and bootstrapped using 100 bootstrap
623 replicates. Node numbers indicate bootstrap branch support ≥ 60 . OTUs retrieved in this
624 study are displayed in bold. Genebank accession numbers for the sequences at individual
625 node tips are given in parentheses. The scale bar displays 0.2 changes per amino acid
626 position.



628 **Figure 3.** Community composition of methane-oxidising bacteria (methanotrophs) of
629 mounds and adjoining soils. a) The non-metric multidimensional scaling (nMDS)
630 ordination shows the methanotrophic community structure (beta diversity) measured by
631 weighted UniFrac distance metric of the *pmoA* gene. The plot further differentiates the
632 methanotroph communities according to termite species and sample location. b)
633 Heatmap showing the relative abundance of the *pmoA* OTUs in all samples. OTUs are
634 ordered according to their position on the phylogenetic tree shown in Figure 3. Differential
635 abundance of *pmoA* OTUs between sample groups was assessed from negative binomial
636 models of the OTU read counts; *p* values were corrected with the false discovery rate
637 approach to account for multiple testing. Only significant tests are shown.



639 **Figure 4.** *In situ* kinetic parameters of methane oxidation in termite mounds. a) Optimal
640 Michaelis-Menten (M-M) curve estimated for a combined data set of *in situ* concentrations
641 and reaction rates from 18 out of 29 mounds showing M-M behavior, excluding 11
642 mounds with an apparent linear increase of rates based on AIC. b) Individual M-M
643 parameters of the 18 mounds showing M-M behavior, including their mean and standard
644 error, and the optimal M-M parameters of the combined data set. c) Positive correlation
645 of activity coefficients k with *pmoA* gene abundance in mound core samples of the 17
646 mounds selected for detailed analysis ($R^2 = 0.44$, $p = 0.0069$). Two outliers have been
647 removed, indicated with red X.

